◆ Human Brain Mapping 37:621–631 (2016) ◆

Dopamine Transporter Availability in Clinically Normal Aging Is Associated With Individual Differences in White Matter Integrity

Anna Rieckmann,[1,2]* Trey Hedden,[1,3] Alayna P. Younger,[1] Reisa A. Sperling,[1,4,5] Keith A. Johnson,[3,4,6] and Randy L. Buckner[1,3,7,8]

[1]Department of Radiology, Massachusetts General Hospital, Athinoula A. Martinos Center for Biomedical Imaging, Charlestown, Massachusetts
[2]Department of Radiation Sciences, Diagnostic Radiology, Umeå University, Umeå, Sweden
[3]Department of Radiology, Massachusetts General Hospital, Harvard Medical School, Boston, Massachusetts
[4]Department of Neurology, Massachusetts General Hospital, Harvard Medical School, Boston, Massachusetts
[5]Department of Neurology, Brigham and Women's Hospital, Harvard Medical School, Center for Alzheimer Research and Treatment, Boston, Massachusetts
[6]Division of Nuclear Medicine and Molecular Imaging, Massachusetts General Hospital, Harvard Medical School, Boston, Massachusetts
[7]Department of Psychiatry, Massachusetts General Hospital, Harvard Medical School, Boston, Massachusetts
[8]Department of Psychology and Center for Brain Science, Harvard University, Cambridge, Massachusetts

Abstract: Aging-related differences in white matter integrity, the presence of amyloid plaques, and density of biomarkers indicative of dopamine functions can be detected and quantified with in vivo human imaging. The primary aim of the present study was to investigate whether these imaging-based measures constitute independent imaging biomarkers in older adults, which would speak to the hypothesis that the aging brain is characterized by multiple independent neurobiological cascades. We assessed MRI-based markers of white matter integrity and PET-based marker of dopamine transporter density and amyloid deposition in the same set of 53 clinically normal individuals (age 65–87). A multiple regression analysis demonstrated that dopamine transporter availability is predicted by white matter integrity, which was detectable even after controlling for chronological age. Further post-hoc

Additional Supporting Information may be found in the online version of this article.

Contract grant sponsor: National Institute on Aging, National Institutes of Health; Contract grant numbers: P01AG036694, R01AG034556, R01AG046396, R01AG037497, K01AG040197, P50AG005134; Contract grant sponsor: Alzheimer's Association; Contract grant number: ZEN-10-174210; Contract grant sponsor: National Institute of Biomedical Imaging and Bioengineering, National Institutes of Health; Contract grant number: P41EB015896; Contract grant sponsor: National Institutes of Health Shared Instrumentation Grant Program and/or High-End Instrumentation Grant Program; Contract grant numbers: S10RR023401, S10RR023043, P41RR014075; Contract grant sponsor: Seventh Framework Programme; Contract grant number: FP7-PEOPLE-2011-IOF (to A.R.) 300217

*Correspondence to: Randy Buckner, Department of Psychology and Center for Brain Science, 52 Oxford Street, Cambridge, MA 02138, USA. E-mail: randy_buckner@harvard.edu

Received for publication 20 June 2015; Revised 26 October 2015; Accepted 28 October 2015.

DOI: 10.1002/hbm.23054
Published online 6 November 2015 in Wiley Online Library (wileyonlinelibrary.com).

exploration revealed that dopamine transporter availability was further associated with systolic blood pressure, mirroring the established association between cardiovascular health and white matter integrity. Dopamine transporter availability was not associated with the presence of amyloid burden. Neurobiological correlates of dopamine transporter measures in aging are therefore likely unrelated to Alzheimer's disease but are aligned with white matter integrity and cardiovascular risk. More generally, these results suggest that two common imaging markers of the aging brain that are typically investigated separately do not reflect independent neurobiological processes. *Hum Brain Mapp 37:621–631, 2016*.

Key words: dopamine; white matter; amyloid; aging; magnetic resonance imaging; positron emission tomography

INTRODUCTION

In vivo human imaging is able to identify prominent aging-related differences in brain biomarkers of white matter integrity, the presence of amyloid plaques and neurotransmitter functions, even in the absence of a clinically diagnosed neurological disorder. Because of the expense and methodological difficulties required for multimodal imaging studies, however, the majority of human imaging studies of the aging brain have relied on a single neurobiological marker, which has led to largely parallel research lines investigating the functional implications of specific neurobiological cascades.

Comparisons across studies suggest that white matter integrity, accumulation of amyloid plaques, and neurotransmitter cell loss, in particular of the dopamine system, may arise from dissociable mechanisms [Buckner, 2004; Hedden and Gabrieli, 2004; Jagust, 2013]. Imaging measures of white matter integrity correlate with cardiovascular risk factors including hypertension and risk for stroke [Breteler et al., 1994; Debette and Markus, 2010; Englund et al., 2004; Fazekas et al., 1993; Jagust et al., 2008; Longstreth et al., 1996]. Elevated amyloid burden is a biomarker of the amyloid plaques that are a hallmark of Alzheimer's disease (AD) and is detectable in a subset of clinically normal older adults who are at high risk to develop AD [Klunk, 2011; Rabinovici and Jagust, 2009; Sojkova and Resnick, 2011; Sperling et al., 2011]. Cross-sectional imaging studies that have investigated imaging markers of white matter damage and amyloid deposition in the same set of individuals have found these markers to be independent [Hedden et al., 2012a,b, 2014; Marchant et al., 2012; Rutten-Jacobs et al., 2011].

Imaging studies of the human dopamine system have suggested reduced density of molecular markers at 5–10% per decade starting from middle age [e.g., Volkow et al., 1996, 1998]. However, there is considerable variability around the estimates of this trajectory. Particularly in adults over the age of 60, some studies have reported a less steep decrease of dopamine markers compared to the estimates for middle adulthood [Cham et al., 2008; Mozley et al., 1999]. Post-mortem studies have confirmed notable loss of nigrostriatal dopamine neurons in clinically normal older adults [Fearnley and Lees, 1991] and both presynaptic dopamine transporter (DAT) markers and postsynaptic receptor markers show relations with cognitive performance in aging [Bäckman et al., 2006; Li et al., 2010]. Little is known about risk factors and neurobiological correlates of molecular markers of the dopamine system in clinically normal aging. The primary aim of the present study was to investigate whether imaging-based measures of the dopamine system constitute a cascade independent of changes in white matter integrity and amyloid accumulation. We consider this investigation important because the results influence how we frame aging-related neurobiological cascades in cross-sectional studies of normal brain aging and interpret studies that focus on functional implications of single imaging markers.

Data are presented from 53 clinically normal older adults who underwent a magnetic resonance imaging (MRI) scan and two positron emission tomography (PET) scans to characterize this sample in terms of white matter integrity, amyloid burden and presynaptic DAT availability. White matter integrity was assessed as white matter hyperintensities (WMH) on a T2-weighted MRI scan and as fractional anisotropy (FA) on a diffusion tensor image (DTI). Amyloid burden was measured as 11C-PIB binding in a large cortical areas and DAT availability was measured as 11C-Altropane binding in striatum.

To foreshadow the main results of this study, a multiple regression analysis revealed that striatal DAT availability was associated with measures of white matter integrity, even after accounting for their shared association with chronological age. We replicate this association in an independent sample that used a different molecular marker of the dopamine system and present two further analyses to better understand the relation. First, we investigate whether the association between DAT availability and white matter integrity was specific to white matter or reflective of a more general association between striatal PET signal and measures of brain structural integrity [i.e., partial volume effects (PVE)]. For this purpose, MRI-based measures of cortical and subcortical atrophy and measures of striatal microstructure (T1 signal inhomogeneity and a

T2-weighted index of striatal iron accumulation) were computed. Second, we investigate whether an association between DAT availability and white matter integrity could be explained by common risk factors. Here, we specifically investigate high blood pressure, as it is an established risk factor for WMH and common in clinically normal older adults.

MATERIAL AND METHODS

Participants

The sample consisted of 53 community-dwelling and clinically normal older adults (28 female), who were recruited as part of the larger Harvard Aging Brain Study [Dagley et al., 2015]. Participants were well educated, with high average estimated verbal IQ rating and high socioeconomic status (Table I). The Clinical Dementia Rating (CDR) scale was administered by a trained neuropsychologist at the time of study enrollment in a semi-structured interview probing six domains of cognitive and functional performance associated with AD, and corroborated by an independent collateral source [Morris, 1993]. All participants were non-demented (CDR = 0). Thirty-three subjects reported current use of anti-hypertensive medication for treatment of hypertension as prescribed by their physician. Systolic blood pressure (BP) was assessed at study enrollment (data missing for three subjects). Subjects with a history of neurological or psychiatric disease or who were found ineligible for MRI were excluded. In addition, a radiologist reviewed MRI images to rule out cortical infarcts, tumor, or other brain abnormalities. All experimental procedures were performed with the understanding and written consent of the subject and the study was approved by the Partners Human Research Committee.

Procedure

Participants completed one 11C-Altropane PET scan, one 11C-PIB PET scan and one MRI session over a period of several months (mean = 8.36, range 1–18 months).

The 11C-Altropane PET scan was used to measure striatal DAT availability [Fischman et al., 2001]. Quantification of available DAT binding sites using PET is a marker of the pathological state of striatal dopamine neurons in numerous disorders including Parkinson's disease [Brooks and Pavese, 2011]. DAT availability in human brain is consistent with known dopaminergic pathways and is most dense in striatal presynaptic dopamine terminals.

The 11C-PIB scan was used to assess amyloid burden. 11C-PIB binds to fibrillar amyloid in cortex, and is a marker of the pathological amyloid deposition associated with AD [Klunk et al., 2004].

Four MRI sequences that were acquired in the same MRI session were utilized in this study. A fluid-attenuated recovery inversion (FLAIR) scan was used to compute WMH, and a DTI scan to estimate voxelwise FA. WMH and FA were used as measures of white matter integrity and included in the analyses of primary interest, which addressed whether striatal DAT availability is predicted by white matter integrity and/or amyloid accumulation. A secondary control analysis explored effects of brain structure on the PET estimates. For this purpose, whole brain, ventricular volumes and striatal signal properties were derived from a T1-weighted multi-echo MPRAGE and a T2-weighted SPACE structural scan. The analyses for each modality are described in detail below.

TABLE I. Sample descriptive

	Mean	Range
Age	75.6	65–87
Education (years)	15.5	8–20
Verbal IQ	121.2	89–132
Socioeconomic status	30.8	11–69
Systolic BP	141.9	109–170, $N = 50$
Diastolic BP	76.2	55–104, $N = 50$

Sample descriptive. Verbal IQ was based on the American National Reading Test [Ryan and Paolo, 1992]. Socioeconomic status was rated on a scale from 11 to 77 with lower scores indicating a higher status [Hollingshead, 1957].

PET Assessments and Analysis

Both PET scans were acquired with an HR+ (CTI, Knoxville, TN) PET camera (3D mode, 63 adjacent slices of 2.42 mm interval, 15.2 cm axial field of view, 5.60 mm transaxial resolution) at Massachusetts General Hospital. At each scan, approximately 15 mCi of the radioligand was intravenously administered as a bolus over 20–30 s. Dynamic images were acquired in 39 frames of increasing duration for a total of 60 min (8×5 s, 4×1 min, 27×2 min). PET data were reconstructed using a filtered back-projection algorithm. Prior to the emission scans, a transmission scan of 10 min was performed and photon attenuation measurements were used to correct the emission data. The participant's head was stabilized using a beaded cushion and velcro straps. Correction for residual head motion was performed on the dynamic data frame forward and backward to a common reference frame (frame 20) before further processing. Dynamic data from the first 8 min were averaged to create an initial uptake image. The initial uptake image was used for normalization of native PET space to a standard MNI PET template. Then, emission data were coregistered to standard space using the normalization parameters obtained from the initial uptake image. The pipeline is illustrated for an 11C-Altropane scan in Figure 1A–C. Spatial normalizations were performed in SPM8 by a two-step procedure of an initial 12-parameter affine transformation followed by non-linear warping (http://www.fil.ion.ucl.ac.uk/spm/software/

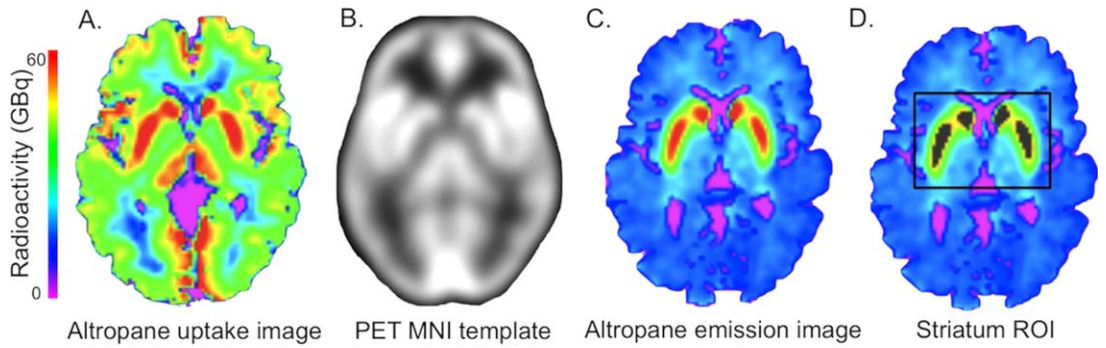

Figure 1.

PET analysis. Summed uptake images (0–8 min, **A**) were normalized to the PET MNI image (**B**), and the normalization parameters applied to the summed emission image (**C**). The striatum region of interest was defined as 1,000 voxels with peak radioactivity (**D**). The ROI is shown in grey on the summed image, with the box surrounding it displaying the search area for the top 1,000. [Color figure can be viewed in the online issue, which is available at wileyonlinelibrary.com.]

spm8/). Radioactivity concentration C was estimated as a function of time t for a given region of interest (ROI) and for the cerebellum, which was used as a reference region for both tracers. The cumulative integral of the reference region curve was plotted against the cumulative integral of the ROI curve (normalized by C_t). The DVR corresponds to the slope of this function for a time window at which the function is linear, in this case 40–60 min [Logan et al., 1990]. Graphical analysis methods with reference region cerebellum have been validated against plasma-input methods for 11C-Altropane [Fischman et al., 2001] and 11C-PIB [Price et al., 2005].

Analyses Specific to 11C-Altropane Data

Voxelwise PVE correction of the 11C-Altropane images was implemented using PVElab Software [Quarantelli et al., 2004) with SPM5 (http://www.fil.ion.ucl.ac.uk/spm/software/spm5] prior to the normalization step. For partial volume correction, the PET and T1-weighted MRI images were co-registered, the T1-image segmented into brain and nonbrain, resliced to the PET voxel size and convolved with an 8-mm point spread function. The dynamic PET images were then corrected using the convolved tissue image on a voxel-by-voxel basis following the methods described by Meltzer et al. (1990). For the 11C-Altropane data, the ROI was the striatum. While spatial normalization of PET images for automatic ROI delineation works reasonably well for cortex, ventricular enlargement can significantly affect the accuracy of spatial normalization for striatum [Reig et al., 2007]. An alternative method for ROI delineation of striatum is manual or automatic delineation in native PET or MRI space. However, anatomical ROI estimates can be inaccurate due to low spatial resolution or low contrast and also differ in size between individuals, which may introduce dependencies between volume measures and DVR. Here, we defined a striatal ROI as the 1,000 voxels with the highest signal intensity on the average emission image. A central cerebellar region of 1,000 voxels was defined in standard space as a reference region. The search for the top 1,000 voxels in striatum was restricted to a large area around the striatum, fit in standard space. This approach ensured that DVR estimation for striatum was fully automated, of a fixed size, and not affected by moderate errors in the registration to standard space. An example of an ROI and the search area is shown in Figure 1D. Even though this approach does not distinguish between subregions of the striatum it accurately separates dopamine transporter densities in clinically normal aging from pathological dopamine loss (Supporting Information 1).

Analyses Specific to 11C-PIB Data

For the PIB data, the ROI was a large cortical region including frontal, lateral parietal and temporal, and retrosplenial cortices (the FLR region). PIB retention in the FLR ROI is substantial in patients with diagnosed AD and has been used as a summary measure amyloid burden in previous studies [Gomperts et al., 2008; Hedden et al., 2009, 2012a; Johnson et al., 2007]. The FLR ROI was defined on the spatially normalized PET image as an aggregate of 60 Anatomical Automatic Labeling (AAL) regions. Cerebellum was also defined by this atlas.

MRI Assessments and Analyses

MRI scans were acquired on a Siemens Tim Trio 3T MRI scanner using a 12-channel head coil at the Athinoula A. Martinos Center for Biomedical Imaging, Massachusetts General Hospital.

WMH Analysis

A FLAIR scan (TR = 6,000 ms, TE = 454 ms, 1 × 1 × 1.5 mm^3 voxels) was used to compute WMH. WMH were calculated on skull-stripped images [Smith, 2002] using methods previously described [Wu et al., 2006]. Briefly, initiating WMH seed regions were identified based on the intensity histogram of the image and iteratively updated. From the resulting WMH segmentation the total WMH volume in mm^3 was estimated within a mask defined by the Johns Hopkins University White Matter Atlas [Wakana et al., 2004], which was reverse normalized to the native space of each individual's FLAIR image.

FA Analysis

DTI images were acquired with a standard DTI sequence with 30 diffusion encoding gradient directions (TR = 8,040 ms, TE = 84 ms, TI = 2,100 ms, 2 × 2 × 2 mm^3 voxels, 64 transverse slices, *b*-value = 700 s mm^{-2}). Processing of DTI data was performed in FSL v5.0.1 using FSL's TBSS [Smith et al., 2006]. Diffusion images were corrected for eddy current distortions and simple head motion by affine registration to the first B0 volume, and the diffusion tensor model was fitted on skull-stripped images at each voxel to generate fractional anisotropy (FA) maps. FA images were registered to the FMRIB58 FA image using a nonlinear transform and normalized FA images from all individuals were averaged to create a sample-specific white matter skeleton [Smith et al., 2006]. Associations between FA and DAT density were computed voxelwise in a general linear model, with and without WMH as a covariate.

Analysis of Brain Volumes and Striatal Signal Properties

A T1-weighted structural scan (TR = 2,200 ms, TI = 1,100 ms, Image1 TE = 1.54 ms, Image2 TE = 3.36 ms, Image3 TE = 5.18 ms, Image4 TE = 7.01 ms, 1.20 mm isotropic voxel size) and a T2 SPACE image (TR = 2,800 ms, TE = 327 ms, 1.20 mm isotropic voxel size) were used to explore and correct the potential for PVE in a post-hoc analysis of the 11C-Altropane data. Estimates of whole brain volume (grey matter + white matter), lateral ventricular volume and estimated total intracranial volume were derived from the T1-weighted images. The volumes were computed following an automated cortical reconstruction and volumetric segmentation performed with the Freesurfer image analysis suite (v 5.1.0; Fischl et al., 2002). Whole brain volume and ventricular volume were adjusted for estimated total intracranial volume following the methods discussed in Buckner et al. (2004).

To investigate possible microstructural contributions to the Altropane PET signal, we computed the standard deviation of the T1 intensity and the mean T2 intensity in the putamen (identified in the Freesurfer segmentation). Subcortical T1 hypointensities are commonly observed on MRI images in older adults and may reflect small lesions. Putamen intensity variation on the T1-weighted image therefore served as one gross, but imperfect, measure of microstructural integrity. Another common striatal microstructural characteristic of aging and possible neurological disorder is iron deposition. There is an established association between excess iron deposition in dopaminergic neurons and Parkinson's disease [Berg et al., 2001] but it has also been associated with AD, multiple sclerosis [Stankiewicz et al., 2007] and WMH [Yan et al., 2013]. Mean T2 SPACE intensity has previously been shown to be a correlate of brain iron concentration [Rossi et al., 2010] and was used in the current study to investigate the association between putamen iron deposition and striatal DAT availability. Similar to the methods described by Rossi et al. we computed mean T2 signal intensity on the SPACE image, normalized to the intensity of white matter using the white matter mask derived in the FreeSurfer segmentation.

Data Transformations and Distributions

WMH, Altropane DVR in striatum, and PIB DVR in the FLR region were used as measures of white matter integrity, DAT availability, and amyloid burden, respectively. The normality of each distribution was tested using the Shapiro–Wilk statistic [Shapiro and Wilk, 1965]. DVR of Altropane was normally distributed ($P = 0.75$). WMH were not ($P < 0.01$), but could be log-transformed into a normal distribution ($P = 0.41$). Altropane DVR values and log-transformed WMH were used as continuous variables in further analyses.

As the FLR DVR estimates for PIB were neither normal ($P < 0.01$) nor log-normal ($P < 0.01$ for both groups), normal mixture modeling (http://cran.r-project.org/web/packages/mclust/index.html) was used to identify the distribution of the PIB DVR data in the clinically normal participants. The data were best described by two distributions and all subjects were allocated to one of the distributions with a probability of ≥ 85%. Based on this analysis, subjects were classified as high or low amyloid burden for further analyses (high amyloid burden: $N = 11$, range = 1.43–1.70, low amyloid burden: $N = 42$, range = 1.02–1.33). A study that has used this approach in a larger sample of subjects established the cut-off for high amyloid burden to be lower (≥1.20) than the distribution of the current sample of clinically normal subjects [Mormino et al., 2014]; see Supporting Information at http://www.neurology.org/content/82/20/1760/suppl/DC1). Based on the lower cut-off of ≥1.20 for high amyloid burden, 4 of the 53 subjects would receive a different classification. Notably, using the lower threshold of ≥1.20 as a cut-off for high amyloid had no impact on the results that we present in relation to amyloid burden below.

Statistical Analysis

The association of white matter integrity and amyloid burden with DAT availability was explored in three consecutive regression models. The first analysis explored whether WMH and PIB status were significant predictors of Altropane DVR in a multiple regression analysis including age as a covariate. Informed by the results, which found that WMH were a significant predictor of Altropane DVR, two follow-up models were computed. In the first, we explored whether the association between Altropane DVR and WMH was reflective of a shared association of both imaging biomarkers with brain structure or striatal microstructure, which could suggest a methodological confound of these methods that introduces an association. For this purpose, we recomputed the primary regression model with four additional variables whole brain volume, ventricle volume, striatal T1 signal inhomogeneity and striatal mean T2 signal. In the final multiple regression model, we test whether the association between Altropane DVR and WMH is explained by common risk factors rather than methodological confounds. Here, we specifically test whether indicators of hypertension (systolic blood pressure and hypertensive medication status), which is a known risk factor for WMH, are related to Altropane DVR and explain the cross-sectional associations between the two imaging markers. The significance threshold for the multiple regression analyses was set to $P = 0.017$ (two-tailed) throughout, controlling for the three sets of analyses. Sex was included as a covariate in all analyses.

Two complimentary analyses are presented to address the generalizability of our findings by testing whether the association between Altropane DVR and WMH holds for different markers of the dopamine system and white matter integrity. First, we tested whether DAT availability was related to microstructural measures of white matter integrity (FA) in a voxelwise general linear model (significance level set to $P < 0.05$, controlling for multiple comparisons using threshold-free cluster enhancement). Second, we explored whether the association between WMH and a molecular marker of the dopamine system replicates and extends to an independent sample that was characterized with a postsynaptic dopamine (D1) receptor ligand. This supplementary analysis included reanalyzing data from a sample of 20 older adults, which was collected at Karolinska University Hospital as part of an independent study (Supporting Information 2).

RESULTS

White Matter Integrity Predicts DAT Availability in Clinically Normal Older Adults

Chronological age significantly predicted DAT availability in this sample (Beta = −0.34, $P = 0.01$). The primary objective of this study was to explore whether striatal DAT availability is an imaging marker of the aged brain that is independent of those imaging markers associated with white matter integrity and accumulation of amyloid in clinically normal older adults. A multiple regression analysis with age, WMH and PIB status as predictors of striatal Altropane DVR revealed that WMH significantly predicted striatal DAT availability (Beta = −0.37, $P = 0.01$, Table II, model 1). For illustration, the univariate association between WMH and Altropane DVR and the partial regression plot from the analysis in model 1 are shown in Figure 2A,B. PIB status did not significantly predict Altropane DVR (Beta = 0.10, $P = 0.47$) and the age association was no longer significant in this model (Beta = −0.18, $P = 0.22$), suggesting that WMH explain, at least in part, aging-related variability in DAT availability.

TABLE II. Regression analysis

Model (R^2)	Predictors of DAT availability	Beta	P
1 (0.19)	WMH	−0.37	0.01
	PIB status	0.10	0.47
	Age	−0.18	0.22
	Sex	−0.11	0.41
2 (0.32)	WMH	−0.42	<0.01
	PIB status	0.18	0.14
	Age	−0.03	0.85
	Whole brain volume	−0.05	0.78
	Ventricular volume	0.07	0.60
	T1 signal inhomogeneity	−0.11	0.39
	T2 signal	0.48	<0.01
	Sex	−0.04	0.77
3 (0.51)	WMH	−0.11	0.41
	PIB status	0.12	0.23
	Age	−0.10	0.46
	T2 signal	0.37	<0.01
	Systolic blood pressure	−0.41	0.01
	Blood pressure medication	−0.22	0.09
	Sex	0.07	0.52

A voxelwise FA analysis also showed that there was a significant and widespread positive association between Altropane DVR and FA ($P < 0.05$, corrected for multiple comparisons; Fig. 2C). The association was not localized to a specific pathway and when WMH were entered as a covariate in the voxelwise analysis, there was no statistically significant association between Altropane DVR and FA. This suggests that the association between white matter integrity and striatal DAT availability is largely driven by the white matter damage that is captured in the WMH count.

The association between WMH and a molecular marker of the striatal dopamine system was replicated in an independent sample of 20 older adults that has been previously described and was re-analyzed for the current study (Supporting Information 2).

Taken together, these findings suggest a robust association between molecular markers of the dopamine system

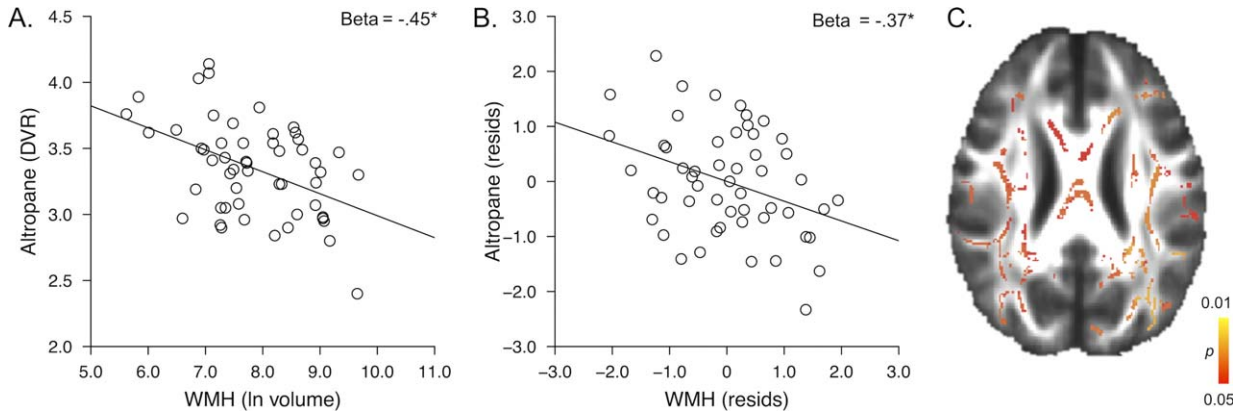

Figure 2.

A. Association between WMH and Altropane DVR. **B**. Residual association between WMH and Altropane DVR, controlling for age and PIB status. **C**. Voxelwise association between Altropane DVR and fractional anisotropy; significant voxels are shown in color ($P < 0.05$, corrected for multiple comparisons). [Color figure can be viewed in the online issue, which is available at wileyonlinelibrary.com.]

and white matter integrity, which was explored in two further analyses.

Control Analysis of Brain Structure

To explore effects of brain structure on Altropane DVR, a control analysis investigated whether Altropane DVR was predicted by whole brain volume, ventricular size or measures of the putamen that are sensitive to microstructural elements, and whether these measures explain the association of Altropane DVR with WMH.

This analysis showed that only lower T2 intensity (a correlate of higher iron concentration) was related to lower Altropane DVR (Beta = 0.48; $P < 0.01$; Table II, model 2). While this effect is important to consider as a possible confounding variable in future studies, in the present study T2 intensity had no substantial influence on the association between WMH and Altropane DVR (Beta = −0.42, $P < 0.01$).

WMH and Dopamine Transporter Availability Share an Association With Systolic BP

The final model again included WMH and PIB status as the main predictors of interest for DAT availability. In addition to age and putamen T2 intensity (identified in model 2) as covariates, this model also included systolic BP and hypertensive medication status. Systolic BP significantly predicted Altropane DVR (Beta = −0.41, $P = 0.01$; Table II, model 3) and hypertensive medication status was related to Altropane DVR at trend-level (Beta = −0.22, $P = 0.09$). In this model, WMH were no longer a significant predictor of Altropane DVR, suggesting that the association between WMH and Altropane DVR was, in part, explained by their shared association with systolic BP and hypertensive medication.

Note, it is unlikely that the association between systolic BP and Altropane DVR reflects a more general association between systolic BP and radiotracer input, as systolic BP was not associated with the integral of the radioactivity curves for either striatum ($r = -0.12$, $P = 0.40$) or cerebellum ($r = 0.01$, $P = 0.97$).

DISCUSSION

In this multi-modal imaging study, white matter integrity, amyloid burden and DAT availability were assessed in the same individuals to examine the cross-sectional association among these imaging biomarkers. In planned tests, we found that white matter integrity significantly predicted striatal DAT availability. Amyloid burden had no association with striatal DAT.

Providing insight into the association between white matter integrity and DAT availability, further post-hoc explorations showed that systolic BP was associated with DAT availability, mirroring the established association between a cardiovascular risk factor and WMH, and explaining much of the relation between the two biomarkers. These results are important because they illustrate that two imaging markers of the aging brain that are typically investigated separately do not reflect independent neurobiological processes. These results influence how we frame age-related neurobiological cascades in cross-sectional studies of normal brain aging, specifically when investigating their effects on behavioral outcomes including domains of cognitive function [Buckner, 2004; Hedden and Gabrieli, 2004; Jagust, 2013]. Perhaps most intriguing though are the questions these results open up for future research in exploring

potential mechanisms that link molecular markers of the dopamine system and white matter integrity in aging, which are discussed in greater detail below.

DAT Availability and White Matter Integrity are Related by a Biological Mechanism

It is biologically plausible that dopamine neurons are particularly vulnerable to hemodynamic abnormalities. Hypertension is associated with elevated cellular calcium influx, and the activity of nigrostriatal dopamine neurons is dependent on calcium channels [Chan et al., 2007; Surmeier, 2007]. Within this possibility, integrity of dopamine neurons and white matter are both jointly affected by hypertension but are not related to each other in a causal chain of events. While this model is consistent with our observations relating to the presynaptic DAT, we note that we were also able to replicate the association between a PET marker of the dopamine system and white matter integrity in an independent sample with PET imaging of the postsynaptic D1 receptor that is found on medium spiny neurons of the striatum (Supporting Information 2). This may suggest that our findings describe a more general relationship between cardiovascular disease and synaptic integrity and are not specific to presynaptic dopamine markers.

High blood pressure over many years compromises brain vasculature, which increases the risk for ischemic events (brief interruptions of blood supply to the brain that result in neuronal injury). When neurons are injured, degeneration of the axon typically precedes the degeneration of the cell body, a process known as "dying back" [Raff et al., 2002]. This suggests one possible mechanism by which hypertension could be causally linked to white matter degeneration and in turn to global synaptic dysfunction, and may relate to the finding that vascular disease exacerbates motor impairments in older patients with Parkinson's disease [Kotagal et al., 2014]. However, considering that dopamine loss is common already in middle adulthood [Cham et al., 2008], prior to the onset of aging-related cardiovascular disease, this interpretation is only reconcilable with the idea of a dual process model: aging-related loss of dopamine functions are determined by "normal" (or, as of now, unexplained) processes starting in the 30s and, in addition, by cardiovascular risk factors in older age.

To better understand the sequence of events across adulthood, longitudinal studies will be of particular value. In fact, an opposite sequence of events, DAT availability predicting the development of hypertension, is also possible. PET studies in young adults have found decreased dopamine receptor availability in smokers [Fehr et al., 2008] and in individuals with higher BMI [Wang et al., 2001], reflecting lifestyle factors associated with the development of hypertension and cardiovascular disease later in life.

DAT Availability and White Matter Integrity are Related by a Secondary Cause

While it is intuitive to look for causal biological mechanisms that can provide an explanation for the observed associations, it is also possible that cross-sectional interrelations between seemingly different brain biomarkers may be an epiphenomenon of normal aging. We removed "aging" from the analysis by covarying for chronological age but chronological age may not be a perfect indicator of brain aging. At present, measures of white matter integrity may be among the best imaging markers to detect individual differences in brain health in older adults as they show reliable correlates to behavioral outcomes in aging [DeCarli et al., 1995; Gunning-Dixon and Raz, 2000; Hedden et al., 2014]. It is possible that many biomarkers of brain aging will correlate to some extent with measures of white matter integrity, beyond chronological age and particularly so in cross-sectional designs, even if they are not mechanistically related [Lindenberger et al., 2011]. Hypotheses regarding brain aging have often focused on the heterogeneity that characterizes brain aging and how different cascades may independently contribute to behavioral outcomes [Buckner, 2004; Hedden and Gabrieli, 2004]. With imaging methods now developed to a point where it is possible to begin to separate normal aging from preclinical disease [Jagust, 2013], we may begin to see that brain biomarkers in aging, absent those likely indicative of preclinical Alzheimer's disease, are instead characterized by an increasing dedifferentiation. The concept of dedifferentiation has also been evoked to describe increasing correlations among behavioral measures in aging [Baltes et al., 1980]. In this way, it is also likely that our findings are not specific to the dopamine system, and that our results would generalize to other markers of neuronal integrity in aging.

LIMITATIONS

We explored the possibility that PVE influence the PET results using a voxelwise correction for CSF contamination as well as control analyses of relations between PET DVR estimates and global atrophy/MRI-based measures of putamen microstructure. We found no evidence for an association between DAT availability and measures of atrophy, and were able to replicate the relation to WMH in an independent sample that used a different PET method. Nevertheless, it remains a possibility that our measure of DAT availability is confounded by PVE, particularly for those adults with smaller striata, for which a proportionally larger area is selected by the top 1000 voxels. Similarly, we cannot completely rule out the possibility that microstructural abnormalities in striatum that remain undetected on MRI affect the PET signal and thereby spuriously introduce an association between cardiovascular risk and striatal DAT availability. There is related evidence

that changes in white matter integrity are associated with changes in blood brain barrier permeability, which may have systematic effects on radioligand binding estimates that we are not able to assess in the current study [Folkersma et al., 2009]. While these potential methodological confounds are serious and require careful further exploration, they do not distract from the main finding of this study that two imaging biomarkers of the aging brain that are commonly used, and typically investigated separately, are in part measuring the same neurobiological cascade.

The strength and novelty of the current study are found in comparisons between multiple PET and MRI imaging markers but these analyses also warrant large sample sizes that justify the multivariate approach. Adequate sample sizes are difficult to attain in these kinds of studies given the high costs in both money and time, as well as a considerable burden placed on the participants. With MRI and PET data becoming more widely available through data sharing and public databases we hope that larger samples are generated in the near future which will allow for replication of our results in a larger cohort.

CONCLUSIONS

This study provides novel evidence for an association between a measure of white matter health and a measure of dopamine synaptic function. On examining possible shared mechanisms between DAT availability and white matter integrity we found that cardiovascular risk factors likely account for the shared variance. These associations were independent of individual differences in amyloid burden, one marker of preclinical Alzheimer's disease. These findings reveal that two commonly studied imaging biomarkers of brain aging previously investigated as separate neurobiological cascades of brain aging are in part related. Further research is needed into the mechanisms by which white matter differences are linked to dopamine synaptic dysfunction.

ACKNOWLEDGMENTS

This research was carried out in whole or in part at the Athinoula A. Martinos Center for Biomedical Imaging at the Massachusetts General Hospital, using resources provided by the Center for Functional Neuroimaging Technologies. The authors thank John H Growdon and Stephen N Gomperts for providing the patient data in Supporting Information 1 and Lars Bäckman for providing the data for the replication sample in Supporting Information 2. The Massachusetts General Hospital Molecular Imaging PET Core provided assistance with PET Imaging and we thank J Alex Becker, Elizabeth Mormino, and Aaron Schultz for assistance during data analysis. Data were collected in collaboration with contributors to the Harvard Aging Brain Study (http://www.martinos.org/harvardagingbrain/Acknowledgements.html).

REFERENCES

Bäckman L, Nyberg L, Lindenberger U, Li S-C, Farde L (2006): The correlative triad among aging, dopamine, and cognition: Current status and future prospects. Neurosci Biobehav Rev 30:791–807.

Baltes PB, Cornelius SW, Spiro A, Nesselroade JR, Willis SL (1980): Integration versus differentiation of fluid/crytallized intelligence in old age. Dev Psychol 16:625–635.

Berg D, Gerlach M, Youdim MBH, Double KL, Zecca L, Riederer P, Becker G (2001): Brain iron pathways and their relevance to Parkinson's disease. J Neurochem 79:225–236.

Breteler MMB, van Swieten JC, Bots ML, Grobbee DE, Claus JJ, van den Hout JHW, van Harskamp F, Tanghe HLJ, de Jong PTVM, van Gijn J, Hofman A (1994): Cerebral white matter lesions, vascular risk factors, and cognitive function in a population-based study: The Rotterdam Study. Neurology 44: 1246–1252.

Brooks DJ, Pavese N (2011): Imaging biomarkers in Parkinson's disease. Prog Neurobiol 95:614–628.

Buckner RL (2004): Memory and executive function in aging and AD: Multiple factors that cause decline and reserve factors that compensate. Neuron 44:195–208.

Buckner RL, Head D, Parker J, Fotenos AF, Marcus D, Morris JC, Snyder AZ (2004): A unified approach for morphometric and functional data analysis in young, old, and demented adults using automated atlas-based head size normalization: Reliability and validation against manual measurement of total intracranial volume. Neuroimage 23:724–738.

Cham R, Studenski SA, Perera S, Bohnen NI (2008): Striatal dopaminergic denervation and gait in healthy adults. Exp Brain Res 185:391–398.

Chan CS, Guzman JN, Ilijic E, Mercer JN, Rick C, Tkatch T, Meredith GE, Surmeier DJ (2007): "Rejuvenation" protects neurons in mouse models of Parkinson's disease. Nature 447:1081–1186.

Dagley A, LaPoint M, Huijbers W, Hedden T, McLaren DG, Chatwal JP, Papp KV, Amariglio RE, Blacker D, Rentz DM, Johnson KA, Sperling RA, Schultz AP (2015) Harvard aging brain study: Dataset and accessibility. Neuroimage. doi: 10.1016/j.neuroimage.2015.03.069. [Epub ahead of print]

Debette S, Markus HS (2010): The clinical importance of white matter hyperintensities on brain magnetic resonance imaging: Systematic review and meta-analysis. BMJ 341:c3666–c3666.

DeCarli C, Murphy DGM, Tranh M, Grady CL, Haxby JV, Gillette JA, Salerno JA, Gonzales-Aviles A, Horwitz B, Rapoport SI, Shapiro MB (1995): The effect of white matter hyperintensity volume on brain structure, cognitive performance, and cerebral metabolism of glucose in 51 healthy adults. Neurology 45: 2077–2084.

Englund E, Sjöbeck M, Brockstedt S, Lätt J, Larsson E-M (2004): Diffusion tensor MRI post mortem demonstrated cerebral white matter pathology. J Neurol 251:350–352.

Fazekas F, Kleinert R, Offenbacher H, Schmidt R, Kleinert G, Payer F, Radner H, Lechner H (1993): Pathologic correlates of incidental MRI white matter signal hyperintensities. Neurology 43:1683–1689.

Fearnley JM, Lees AJ (1991): Ageing and Parkinson's disease: Substantia nigra regional selectivity. Brain 114:2283–2301.

Fehr C, Yakushev I, Hohmann N, Buchholz H-G, Landvogt C, Deckers H, Eberhardt A, Kläger M, Smolka M, Scheurich A, Dielentheis T, Schmidt LG, Rösch F, Bartenstein P, Gründer G,

Schreckenberger M (2008): Association of low striatal dopamine d2 receptor availability with nicotine dependence similar to that seen with other drugs of abuse. Am J Psychiatry 165: 507–514.

Fischl B, Salat DH, Busa E, Albert M, Dieterich M, Haselgrove C, van der Kouwe A, Killiany R, Kennedy D, Klaveness S, Montillo A, Makris N, Rosen B, Dale AM (2002): Whole brain segmentation: Automated labeling of neuroanatomical structures in the human brain. Neuron 33:341–355.

Fischman AJ, Bonab AA, Babich JW, Livni E, Alpert NM, Meltzer PC, Madras BK (2001): [11C, 127I] Altropane: A highly selective ligand for PET imaging of dopamine transporter sites. Synapse 39:332–342.

Folkersma H, Boellaard R, Vandertop WP, Kloet RW, Lubberink M, Lammertsma AA, van Berckel BNM (2009): Reference tissue models and blood-brain barrier disruption: Lessons from (R)-[C-11]PK11195 in traumatic brain injury. J Nucl Med 50: 1975–1979.

Gomperts SN, Rentz DM, Moran E, Becker JA, Locascio JJ, Klunk WE, Mathis CA, Elmaleh DR, Shoup T, Fischman AJ, Hyman BT, Growdon JH, Johnson KA (2008): Imaging amyloid deposition in Lewy body diseases. Neurology 71:903–910.

Gunning-Dixon FM, Raz N (2000): The cognitive correlates of white matter abnormalities in normal aging: A quantitative review. Neuropsychol 14:224–232.

Hedden T, Gabrieli JDE (2004): Insights into the ageing mind: A view from cognitive neuroscience. Nat Rev Neurosci 5:87–96.

Hedden T, Mormino EC, Amariglio RE, Younger AP, Schultz AP, Becker JA, Buckner RL, Johnson KA, Sperling RA, Rentz DM (2012a): Cognitive profile of amyloid burden and white matter hyperintensities in cognitively normal older adults. J Neurosci 32:16233–16242.

Hedden T, Schultz AP, Rieckmann A, Mormino EC, Johnson KA, Sperling RA, Buckner RL (2014) Multiple brain markers are linked to age-related variation in cognition. Cereb Cortex. doi: 10.1093/cercor/bhu238 [Epub ahead of print]

Hedden T, Van Dijk KRA, Becker JA, Mehta A, Sperling RA, Johnson KA, Buckner RL (2009): Disruption of functional connectivity in clinically normal older adults harboring amyloid burden. J Neurosci 29:12686–12694.

Hedden T, Van Dijk KRA, Shire EH, Sperling RA, Johnson KA, Buckner RL (2012b): Failure to modulate attentional control in advanced aging linked to white matter pathology. Cereb Cortex 22:1038–1051.

Hollingshead AB (1957): Two factor index of social position. New Haven: CT. 22p.

Jagust W (2013): Vulnerable neural systems and the borderland of brain aging and neurodegeneration. Neuron 77:219–234.

Jagust WJ, Zheng L, Harvey DJ, Mack WJ, Vinters HV, Weiner MW, Ellis WG, Zarow C, Mungas D, Reed BR, Kramer JH, Schuff N, DeCarli C, Chui HC (2008): Neuropathological basis of magnetic resonance images in aging and dementia. Ann Neurol 63:72–80.

Johnson KA, Gregas M, Becker JA, Kinnecom C, Salat DH, Moran EK, Smith EE, Rosand J, Rentz DM, Klunk WE, Mathis CA, Price JC, DeKosky ST, Fischman AJ, Greenberg SM (2007): Imaging of amyloid burden and distribution in cerebral amyloid angiopathy. Ann Neurol 62:229–234.

Klunk WE (2011): Amyloid imaging as a biomarker for cerebral β-amyloidosis and risk prediction for Alzheimer dementia. Neurobiol Aging 32:S20–S36.

Klunk WE, Engler H, Nordberg A, Wang Y, Blomqvist G, Holt DP, Savitcheva I, Huang GF, Estrada S, Ausén B, Debnath ML, Barletta J, Price JC, Sandell J, Lopresti BJ, Wall A, Koivisto P, Antoni G, Mathis CA, Långström B (2004): Imaging brain amyloid in Alzheimer's disease with Pittsburgh Compound-B. Ann Neurol 55:306–319.

Kotagal V, Albin RA, Müller MLTM, Koeppe RA, Studenski S, Frey KA, Bohnen NI (2014): Advanced age, cardiovascular risk burden, and timed up and go test performance in Parkinson disease. J Gerontol A Biol Sci Med Sci 69:1569–1575.

Li S-C, Lindenberger U, Bäckman L (2010): Dopaminergic modulation of cognition across the life span. Neurosci Biobehav Rev 34:625–630.

Lindenberger U, Oertzen von T, Ghisletta P, Hertzog C (2011): Cross-sectional age variance extraction: What's change got to do with it? Psychol Aging 26:34–47.

Logan J, Fowler JS, Volkow ND, Wolf AP, Dewey SL, Schlyer DJ, MacGregor RR, Hitzemann R, Bendriem B, Gatley SJ, Christman DR (1990): Graphical analysis of reversible radioligand binding from time-activity measurements applied to [*N*−11C-methyl]-(-)-cocaine PET studies in human subjects. J Cereb Blood Flow Metab 10:740–747.

Longstreth WT, Manolio TA, Arnold A, Burke GL, Bryan N, Jungreis CA, Enright PL, O'Leary D, Fried L, for the Cardiovascular Health Study (1996): Clinical correlates of white matter findings on cranial magnetic resonance imaging of 3301 elderly people: The cardiovascular health study. Stroke 27: 1274–1282.

Marchant NL, Reed BR, DeCarli CS, Madison CM, Weiner MW, Chui HC, Jagust WJ (2012): Cerebrovascular disease, beta-amyloid, and cognition in aging. Neurobiol Aging 33:1006.e25–1036.

Meltzer CC, Leal JP, Mayberg HS, Wagner HN, Frost JJ (1990): Correction of PET data for partial volume effects in human cerebral cortex by MR imaging. J Comput Assist Tomogr 14: 561–570.

Mormino EC, Betensky RA, Hedden T, Schultz AP, Ward A, Huijbers W, Rentz DM, Johnson KA, Sperling RA, Alzheimer's Disease Neuroimaging Initiative, Australian Imaging Biomarkers Lifestyle Flagship Study of Ageing, Harvard Aging Brain Study (2014): Amyloid and APOE ϵ4 interact to influence short-term decline in preclinical Alzheimer disease. Neurology 82:1760–1767.

Morris JC (1993): The clinical dementia rating (CDR): Current version and scoring rules. Neurology 43:2412–2414.

Mozley PD, Acton PD, Barraclough ED, Plössl K, Gur RC, Alavi A, Mathur A, Saffer J, Kung HF (1999): Effects of age on dopamine transporters in healthy humans. J Nucl Med 40:1812–1817.

Price JC, Klunk WE, Lopresti BJ, Lu X, Hoge JA, Ziolko SK, Holt DP, Meltzer CC, DeKosky ST, Mathis CA (2005): Kinetic modeling of amyloid binding in humans using PET imaging and Pittsburgh Compound-B. J Cereb Blood Flow Metab 25:1528–1547.

Quarantelli M, Berkouk K, Prinster A, Landeau B, Svarer C, Balkay L, Alfano B, Brunetti A, Baron J-C, Salvatore M (2004): Integrated software for the analysis of brain PET/SPECT studies with partial-volume-effect correction. J Nucl Med 45: 192–201.

Rabinovici GD, Jagust WJ (2009): Amyloid imaging in aging and dementia: Testing the amyloid hypothesis in vivo. Beh Neurol 21:117–128.

Raff MC, Whitmore AV, Finn JT (2002): Axonal self-destruction and neurodegeneration. Science 296:868–871.

Reig S, Penedo M, Gispert JD, Pascau J, Sánchez-González J, García-Barreno P, Desco M (2007): Impact of ventricular enlargement on the measurement of metabolic activity in spatially normalized PET. Neuroimage 35:748–758.

Rossi M, Ruottinen H, Elovaara I, Ryymin P, Soimakallio S, Eskola H, Dastidar P (2010): Brain iron deposition and sequence characteristics in Parkinsonism: Comparison of SWI, T_2* maps, T_2-weighted-, and FLAIR-SPACE. Invest Radiol 45: 795–802.

Rutten-Jacobs LCA, de Leeuw F-E, Geurts-van Bon L, Gordinou de Gouberville MC, Schepens-Franke AN, Dederen PJ, Spliet WGM, Wesseling P, Kiliaan AJ (2011): White matter lesions are not related to β-Amyloid deposition in an autopsy-based study. Curr Gerontol Geriatr Res 2011:1–5.

Ryan JJ, Paolo AM (1992): A screening procedure for estimating premorbid intelligence in the elderly. Clin Neuropsychol 6:53–62.

Shapiro SS, Wilk MB (1965): An analysis of variance test for normality (complete samples). Biometrika 52:591–611.

Smith SM (2002): Fast robust automated brain extraction. Hum Brain Mapp 17:143–155.

Smith SM, Jenkinson M, Johansen-Berg H, Rueckert D, Nichols TE, Mackay CE, Watkins KE, Ciccarelli O, Cader MZ, Matthews PM, Behrens TEJ (2006): Tract-based spatial statistics: Voxelwise analysis of multi-subject diffusion data. Neuroimage 31:1487–1505.

Sojkova J, Resnick MS (2011): In vivo human amyloid imaging. Curr Alzheimers Res 8:366–372.

Sperling RA, Aisen PS, Beckett LA, Bennett DA, Craft S, Fagan AM, Iwatsubo T, Jack CR Jr, Kaye J, Montine TJ, Park DC, Reiman EM, Rowe CC, Siemers E, Stern Y, Yaffe K, Carrillo MC, Thies B, Morrison-Bogorad M, Wagster MV, Phelps CH (2011): Toward defining the preclinical stages of Alzheimer's disease: Recommendations from the National Institute on Aging-Alzheimer's Association workgroups on diagnostic guidelines for Alzheimer's disease. Alzheimers Dement 7:280–292.

Stankiewicz J, Panter SS, Neema M, Arora A, Batt CE, Bakshi R (2007): Iron in chronic brain disorders: Imaging and neurotherapeutic implications. Neurotherapeutics 4:371–386.

Surmeier DJ (2007): Calcium, ageing, and neuronal vulnerability in Parkinson's disease. Lancet Neurol 6:933–938.

Volkow ND, Ding YS, Fowler JS, Wang GJ, Logan J, Gatley SJ, Hitzemann R, Smith G, Fields SD, Gur R (1996): Dopamine transporters decrease with age. J Nucl Med 37:554–559.

Volkow ND, Wang GJ, Fowler JS, Ding YS, Gur RC, Gatley J, Logan J, Moberg PJ, Hitzemann R, Smith G, Pappas N (1998): Parallel loss of presynaptic and postsynaptic dopamine markers in normal aging. Ann Neurol 44:143–147.

Wakana S, Jiang H, Nagae-Poetscher LM, van Zijl PCM, Mori S (2004): Fiber tract-based atlas of human white matter anatomy. Radiology 230:77–87.

Wang G-J, Volkow ND, Logan J, Pappas NR, Wong CT, Zhu W, Netusll N, Fowler JS (2001): Brain dopamine and obesity. Lancet 357:354–357.

Wu M, Rosano C, Butters M, Whyte E, Nable M, Crooks R, Meltzer CC, Reynolds CF, Aizenstein HJ (2006): A fully automated method for quantifying and localizing white matter hyperintensities on MR images. Psychiatry Res 148:133–142.

Yan S, Sun J, Chen Y, Selim M, Lou M (2013): Brain iron deposition in white matter hyperintensities: A 3-T MRI study. AGE 35:1927–1936.